N94-13308

A Model for Rotorcraft Flying Qualities Studies *

Manoj Mittal
Post–Doctoral Fellow
School of Aerospace Engineering

Mark F. Costello
Research Engineer
Aerospace Laboratory, GTRI

Georgia Institute of Technology
Atlanta, Georgia

Abstract

This paper outlines the development of a mathematical model that is expected to be useful for rotorcraft flying qualities research. A computer model is presented that can be applied to a range of different rotorcraft configurations. The algorithm computes vehicle trim and a linear state-space model of the aircraft. The trim algorithm uses non linear optimization theory to solve the non linear algebraic trim equations. The linear aircraft equations consist of an airframe model and a flight control system dynamic model. The airframe model includes coupled rotor and fuselage rigid body dynamics and aerodynamics. The aerodynamic model for the rotors utilizes blade element theory and a three state dynamic inflow model. Aerodynamics of the fuselage and fuselage empennages are included. The linear state-space description for the flight control system is developed using standard block diagram data.

Introduction

In the past, rotorcraft flight control system preliminary design used mathematical models which assumed the fuselage to possess six degrees of freedom. The rotor dynamics were assumed to be substantially faster than the fuselage dynamics and were subsequently approximated as quasi-static. The process of fine tuning the flight control system was accomplished through an extensive flight test program comprised of a matrix of control system parameter variations. While fine tuning of the flight control system is still accomplished through flight testing the vehicle, significant improvements in the optimization process have been realized when high order dynamic rotorcraft models are utilized during the preliminary flight control system design stage.

Rotorcraft are now being designed with sophisticated electronic flight control systems. These complex control systems are utilized not only to satisfy standard flying qualities specifications but also to meet aerodynamic performance, vibration, and structural loads criteria. The design of modern rotorcraft flight control systems now stretches across many different individual disciplines and is indeed interdisciplinary. The general trend toward increased reliance on the flight control system for improving overall system performance has lead designers to consider higher bandwidth systems which rely on high levels of sensor feedback to yield desired aircraft stability. The main drawback of this approach is that increased levels of feedback, which in general improve the low frequency fuselage dynamic behavior, can destabilize higher frequency rotor blade motion. In order to make meaningful estimates of the impact of a particular flight control configuration on system requirements it has been found that a mathematical model which includes fuselage and rotor rigid body dynamics and rotor dynamic inflow is necessary [1].

The business of rotorcraft modeling for flight control system design and analysis support has been an active research area for many years. Deriving the equations of motion of a fully coupled fuselage and rotor system for a reasonably general configuration quickly becomes unwieldy due to complicated geometry including many matrix transformations and intricate logic branching. These complexities have lead engineers to develop digital computer programs which more or less relegate model computation to the computer and free the engineer to focus on analysis results.

Talbot, Tinling, Decker, and Chen [2] formulated a helicopter flying qualities model that includes fuselage dynamics and a three degree of freedom tip-path-plane representation for the main rotor flapping dynamics. Some simplifications are made in the analysis in order to formulate compact, analytical force

*Presented at Piloting Vertical Flight Aircraft: A Conference on Flying Qualities and Human Factors, San Francisco, California, January 1993.

and moment expressions for the rotor forces and moments. Gibbons and Done [3] derived a numerical method to automatically generate rotorcraft equations of motion. The method uses Lagrange's equations and relies on expressing inertial position vectors of the rotor blades as a matrix multiplied by the position vector in blade coordinates plus a term that is a function of the modal coordinates, time, and spanwise position. The required differentiations of the position vector to form the equations of motion are performed numerically. Miller and White [1] used concepts from Lytwyn [4] and Gibbons and Done [3] to automate generation of the equations of motion for rotorcraft handling qualities analysis. Miller and White [1] expressed all transformation matrices in complex variable form and were able to develop a compact algorithm to analytically obtain long strings of orthogonal transformation matrices along with all necessary derivatives to form nonlinear and linearized dynamic equations. Lagrange's equations were used in the formulation. Zhao and Curtiss [5] derived a set of linearized equations by analytic linearization of a nonlinear model formulated using Lagrange's equations. The symbolic manipulation computer program MACSYMA was used in forming the equations. Subsequent work by McKillip and Curtiss [6] has improved and extended the work by Zhao and Curtiss [5].

The work discussed in this paper derives a rotorcraft flying qualities model which has been implemented into a FORTRAN computer program. A fairly generic rotorcraft configuration, consisting of a rigid fuselage, two rotors, and an arbitrary number of fuselage fixed external surfaces has been assumed, as shown in Figure 1. It is important to note that the type of analysis carried out in this work can accommodate any arbitrary number of rotors in the configuration. The number of rotors has been chosen to be two since the majority of rotorcraft fall under this category. The fuselage possesses six degrees of freedom and the rotor blades have flap, lag, and pitch degrees of freedom. The rotor aerodynamic models are based on blade element theory and include three degree of freedom dynamic inflow. The equations of motion are formulated using Kane's equations [7]. More importantly, derivatives of transformation matrices are formed using angular velocity expressions as opposed to numerical or direct differentiation. The rotor dynamic inflow equations are based on the Pitt and Peters model [8] and include hub motion perturbations. The residual of the equations of motion and the residual gradient expressions are derived analytically and trim is calculated using the residual and residual gradients in concert with a modified Newton's method. The rotor trim variables are the rotor multiblade coordinates. A linear constant coefficient model of the composite airframe is formulated using a multiblade coordinate transformation with a subsequent constant coefficient approximation. The linear constant coefficient airframe model is coupled to the linear control system dynamic model to form the overall linear model. Linear analysis tools such as eigen values, eigen vectors, transfer functions, frequency response, and linear simulation are directly contained within the computer program.

Airframe Dynamic Model

As pictured in Figure 1, the airframe dynamic model consists of a rigid fuselage with the standard six degrees of freedom and two fully articulated rotor systems, each with dynamic inflow. The fuselage aerodynamic force and moment components are obtained in the wind axis from a two dimensional data table as functions of fuselage angle of attack and sideslip. The aerodynamic forces exerted on the external surfaces are obtained using standard lifting line theory. The rotor geometry details are shown in Figure 2. Provisions are made in the model to accommodate any of the six possible sequences of flap, lag, and pitch hinges for the rotor blades. Each hinge is accompanied by a linear torsional spring and damper. Each blade also has a non linear translational damper which is attached to the rotor blade from the rotor hub. Hingeless rotor systems can be approximately modeled using a virtual hinge representation. The aerodynamic forces exerted on the rotor blades are calculated using blade element theory. The blades on a rotor have identical yet arbitrary geometric and inertial properties.

The airframe nonlinear dynamic model is obtained using the flat and non-rotating earth assumption. Kane's Equations are then written for each degree of freedom by taking into account the contributions of the generalized inertia forces, the generalized gravity forces, the generalized aerodynamic forces, and the generalized spring-damper forces.

$$f_r(t) = f_{I_r}(t) + f_{G_r}(t) + f_{A_r}(t) + f_{SD_r}(t), \qquad r = 1, \ldots, n_{RB} \quad (1)$$

In equation 1, t denotes time and n_{RB} is the number of generalized speeds. The origin of each term on the right hand side of Equation 1 is discussed below.

The following nomenclature is introduced for deriving the generalized inertia forces. Let n_{R1} and n_{R2} denote the number of blades on rotor 1 and rotor

2, respectively. Let m_F and I_F, $m_{R1,i}$ and $I_{R1,i}$ ($i = 1,\ldots,n_{R1}$), and $m_{R2,j}$ and $I_{R2,j}$ ($j = 1,\ldots,n_{R2}$), respectively, denote the masses and inertia matrices for the fuselage, rotor 1 blades, and rotor 2 blades. Let $\omega_F, \omega_{R1,i}$ ($i = 1,\ldots,n_{R1}$), and $\omega_{R2,j}$ ($j = 1,\ldots,n_{R2}$) represent the individual body axis components of the angular velocities of the fuselage, rotor 1 blades, and rotor 2 blades, respectively. Let v_{F^*} and a_{F^*}, v_{R1,i^*} and a_{R1,i^*} ($i = 1,\ldots,n_{R1}$), and v_{R2,j^*} and a_{R2,j^*} ($j = 1,\ldots,n_{R2}$) represent the inertial axis components of the c.g. (center of gravity) velocities and accelerations of the fuselage, rotor 1 blades, and rotor 2 blades, respectively. Then the generalized inertia forces acting on the configuration can be written as,

$$\begin{aligned} f_{I_r}(t) \;=\;& m_F\left(\frac{\partial v_{F^*}}{\partial u_r}\right)^T a_{F^*} + \\ & \sum_{i=1}^{n_{R1}} m_{R1,i}\left(\frac{\partial v_{R1,i^*}}{\partial u_r}\right)^T a_{R1,i^*} + \\ & \sum_{i=1}^{n_{R2}} m_{R2,i}\left(\frac{\partial v_{R2,i^*}}{\partial u_r}\right)^T a_{R2,i^*} + \\ & \left(\frac{\partial \omega_F}{\partial u_r}\right)^T \{I_F\dot{\omega}_F + S(\omega_F)I_F\omega_F\} + \\ & \sum_{i=1}^{n_{R1}}\left(\frac{\partial \omega_{R1,i}}{\partial u_r}\right)^T \{I_{R1,i}\dot{\omega}_{R1,i} + S(\omega_{R1,i})I_{R1,i}\omega_{R1,i}\} + \\ & \sum_{i=1}^{n_{R2}}\left(\frac{\partial \omega_{R2,i}}{\partial u_r}\right)^T \{I_{R2,i}\dot{\omega}_{R2,i} + S(\omega_{R2,i})I_{R2,i}\omega_{R2,i}\}, \\ & r = 1,\ldots,n_{RB} \qquad (2) \end{aligned}$$

where an overdot denotes differentiation with respect to time and $S(\cdot)$ is the standard cross product skew-symmetric matrix operator (Appendix). u is the vector of generalized speeds. Letting g be the acceleration due to gravity, the generalized gravity forces can be written as,

$$\begin{aligned} f_{G_r}(t) \;=\;& -m_F g\frac{\partial (v_{F^*})_3}{\partial u_r} \\ & -\sum_{i=1}^{n_{R1}} m_{R1,i}g\frac{\partial (v_{R1,i^*})_3}{\partial u_r} \\ & -\sum_{i=1}^{n_{R2}} m_{R2,i}g\frac{\partial (v_{R2,i^*})_3}{\partial u_r}, \\ & r = 1,\ldots,n_{RB} \qquad (3) \end{aligned}$$

The generalized aerodynamic forces are discussed next. Let v_F, and F_F and M_F be respectively the body axis components of the velocity and the aerodynamic force and moment acting on the fuselage aerodynamic center. Let b_{R1}, b_{R2}, and b_{S_i} ($i = 1,\ldots,n_S$) denote the number of elements or sections on any rotor 1 blade, any rotor 2 blade, and the ith external surface. Let $v_{R1,i,j}$ and $F_{R1,i,j}$ ($i = 1,\ldots,n_{R1}, j = 1,\ldots,b_{R1}$), and $v_{R2,k,l}$ and $F_{R2,k,l}$ ($k = 1,\ldots,n_{R2}, l = 1,\ldots,b_{R2}$) be the individual body axis components of the section velocity and the aerodynamic force acting on rotor 1 blades and rotor 2 blades, respectively. Let $v_{S_i,j}$ and $F_{S_i,j}$ ($i = 1,\ldots,n_S, j = 1,\ldots,b_{S_i}$) be the respective body axis components of the section velocity and the aerodynamic force acting on the external surfaces. The generalized aerodynamic forces acting on the configuration can then be written as,

$$\begin{aligned} f_{A_r}(t) \;=\;& -\left\{\left(\frac{\partial v_F}{\partial u_r}\right)^T F_F + \left(\frac{\partial \omega_F}{\partial u_r}\right)^T M_F\right\} \\ & -\sum_{i=1}^{n_{R1}}\sum_{j=1}^{b_{R1}}\left(\frac{\partial v_{R1,i,j}}{\partial u_r}\right)^T F_{R1,i,j} \\ & -\sum_{i=1}^{n_{R2}}\sum_{j=1}^{b_{R2}}\left(\frac{\partial v_{R2,i,j}}{\partial u_r}\right)^T F_{R2,i,j} \\ & -\sum_{i=1}^{n_S}\sum_{j=1}^{b_{S_i}}\left(\frac{\partial v_{S_i,j}}{\partial u_r}\right)^T F_{S_i,j}, \\ & r = 1,\ldots,n_{RB} \qquad (4) \end{aligned}$$

The generalized spring-damper forces are discussed next. Figure 2 shows the typical spring-damper attachment geometry for a typical blade. Let $v^D_{R1,i,j}$ and $F^D_{R1,i,j}$ ($i = 1,\ldots,n_{R1}, j = 1,2$), and $v^D_{R2,k,l}$ and $F^D_{R2,k,l}$ ($k = 1,\ldots,n_{R2}, l = 1,2$) be the individual rotor hub axis components of the velocities and the forces acting on the translational damper attachment points for rotor 1 blades and rotor 2 blades, respectively. Let $\omega^D_{R1,i,j}$ and $M^D_{R1,i,j}$ ($i = 1,\ldots,n_{R1}, j = 1,\ldots,4$), and $\omega^D_{R2,k,l}$ and $M^D_{R2,k,l}$ ($k = 1,\ldots,n_{R2}, l = 1,\ldots,4$) denote the individual body axis components of the angular velocities and the torsional spring-damper moments acting on the hub, link 1, link 2, and the blade for rotor 1 blades and rotor 2 blades, respectively. Then the generalized spring-damper forces can be expressed as,

$$\begin{aligned} f_{SD_r}(t) \;=\;& -\sum_{i=1}^{n_{R1}}\sum_{j=1}^{2}\left(\frac{\partial v^D_{R1,i,j}}{\partial u_r}\right)^T F^D_{R1,i,j} \\ & -\sum_{i=1}^{n_{R2}}\sum_{j=1}^{2}\left(\frac{\partial v^D_{R2,i,j}}{\partial u_r}\right)^T F^D_{R2,i,j} \end{aligned}$$

$$-\sum_{i=1}^{n_{R1}}\sum_{j=1}^{4}\left(\frac{\partial\omega_{R1,i,j}^{D}}{\partial u_r}\right)^T M_{R1,i,j}^{D}$$
$$-\sum_{i=1}^{n_{R2}}\sum_{j=1}^{4}\left(\frac{\partial\omega_{R2,i,j}^{D}}{\partial u_r}\right)^T M_{R2,i,j}^{D},$$
$$r = 1,\ldots,n_{RB} \quad (5)$$

The partial derivatives $\frac{\partial v}{\partial u_r}$ and $\frac{\partial \omega}{\partial u_r}$ in Equations 2 through 5 are known as partial velocities and partial angular velocities, respectively. The generalized coordinate vector q and the generalized speed vector u are defined as follows:

$$\begin{aligned} q &= \{(q_F)^T,(q_{R1,1})^T,(q_{R1,2})^T,\ldots,(q_{R1,n_{R1}})^T, \\ &\quad (q_{R2,1})^T,(q_{R2,2})^T,\ldots,(q_{R2,n_{R2}})^T\}^T \quad (6) \\ u &= \{(u_F)^T,(u_{R1,1})^T,(u_{R1,2})^T,\ldots,(u_{R1,n_{R1}})^T, \\ &\quad (u_{R2,1})^T,(u_{R2,2})^T,\ldots,(u_{R2,n_{R2}})^T\}^T \quad (7) \end{aligned}$$

The subscripts F, $R1$, and $R2$ refer to fuselage, rotor 1, and rotor 2 variables, respectively. Further,

$$q_F = \{x, y, z, \phi, \theta, \psi\}^T \quad (8)$$
$$q_{R1,i} = \{\alpha_{R1,i}^{(1)}, \alpha_{R1,i}^{(2)}, \alpha_{R1,i}^{(3)}\}^T, \quad i = 1,\ldots,n_{R1} \quad (9)$$
$$q_{R2,i} = \{\alpha_{R2,i}^{(1)}, \alpha_{21,i}^{(2)}, \alpha_{R2,i}^{(3)}\}^T, \quad i = 1,\ldots,n_{R2} \quad (10)$$
$$u_F = \{u, v, w, p, q, r\}^T \quad (11)$$
$$u_{R1,i} = \{\dot\alpha_{R1,i}^{(1)}, \dot\alpha_{R1,i}^{(2)}, \dot\alpha_{R1,i}^{(3)}\}^T, \quad i = 1,\ldots,n_{R1} \quad (12)$$
$$u_{R2,i} = \{\dot\alpha_{R2,i}^{(1)}, \dot\alpha_{R2,i}^{(2)}, \dot\alpha_{R2,i}^{(3)}\}^T, \quad i = 1,\ldots,n_{R2} \quad (13)$$

The quantities $\alpha^{(1)}$, $\alpha^{(2)}$, and $\alpha^{(3)}$ are one of lag, flap, and pitch angles, depending on the rotor blade hinge sequence.

A brief description of the analysis involved in calculating the terms on the right hand sides of Equations 2 through 5 is given in the following. For simplicity, the analysis for the rotor terms will be restricted to rotor 1; the analysis for rotor 2 terms is analogous.

Generalized Inertia Forces

The six terms comprising the generalized inertia forces, Equation 2, are discussed here. The orientation of the fuselage with respect to inertial axes and the orientation of the rotors with respect to the fuselage can be described using transformation matrices. Each transformation matrix is composed of one, two, or three single axis transformation matrices. Referring to Figure 2, let T_F be the matrix of transformations from the fuselage axes to inertial axes. The following five matrices are defined for rotor 1. T_{S1} is the matrix of transformations from shaft axes to fuselage axes, $T_{H1,i}$ ($i = 1,\ldots,n_{R1}$) is the matrix of transformations from rotating hub axes to shaft axes, $T_{R1,i}^{(1)}$ ($i = 1,\ldots,n_{R1}$) is the matrix of transformations from link 1 axes to rotating hub axes, $T_{R1,i}^{(2)}$ ($i = 1,\ldots,n_{R1}$) is the matrix of transformations from link 2 axes to link 1 axes, and $T_{R1,i}^{(3)}$ ($i = 1,\ldots,n_{R1}$) is the matrix of transformations from blade axes to link 2 axes. The transformation matrices are expressed as follows:

$$\begin{aligned} T_F &= [E_1(\phi)E_2(\theta)E_3(\psi)]^T && (14) \\ T_{S1} &= [T_{S1,b}(\Gamma_{S1,b})T_{S1,a}(\Gamma_{S1,a})]^T && (15) \\ T_{H1,i} &= [E_3(\pi - \psi_{R1,i})]^T && (16) \\ T_{R1,i}^{(1)} &= T_{R1,i}^{(1)}(\alpha_{R1,i}^{(1)}) && (17) \\ T_{R1,i}^{(2)} &= T_{R1,i}^{(2)}(\alpha_{R1,i}^{(2)}) && (18) \\ T_{R1,i}^{(3)} &= T_{R1,i}^{(3)}(\alpha_{R1,i}^{(3)}) && (19) \end{aligned}$$

In Equation 16, $\psi_{R1,i} = \Omega_{R1}t + \frac{2\pi}{n_{R1}}(i-1)$, where Ω_{R1} is the rotor 1 hub rotational speed. It is assumed that the shaft is inclined with respect to the fuselage by first a rotation with the angle $\Gamma_{S1,a}$ and then a rotation with the angle $\Gamma_{S1,b}$. Depending on the sequence of rotation, $T_{S1,a}$ and $T_{S1,b}$ are one each among E_1 and E_2. E_1, E_2, and E_3 are single axis transformation matrices about x, y, and z axes, respectively (Appendix). Clearly, $T^{(1)}$, $T^{(2)}$, and $T^{(3)}$ are one each among E_1, E_2, and E_3, depending on the rotor blade hinge sequence.

The body axis components of the angular velocity of the fuselage, ω_F, can be written as,

$$\omega_F = \{p, q, r\}^T \quad (20)$$

Using the transformation matrices defined above, the body axis components of the angular velocity of the ith rotor 1 blade can be written as,

$$\begin{aligned} \omega_{R1,i} = & \left[T_{S1}T_{H1,i}T_{R1,i}^{(1)}T_{R1,i}^{(2)}T_{R1,i}^{(3)}\right]^T \omega_F + \\ & \left[T_{R1,i}^{(1)}T_{R1,i}^{(2)}T_{R1,i}^{(3)}\right]^T \{0,0,-\Omega_{R1}\}^T + \\ & \left[T_{R1,i}^{(2)}T_{R1,i}^{(3)}\right]^T b_{R1}^{(1)}\dot\alpha_{R1,i}^{(1)} + \\ & \left[T_{R1,i}^{(3)}\right]^T b_{R1}^{(2)}\dot\alpha_{R1,i}^{(2)} + \\ & b_{R1}^{(3)}\dot\alpha_{R1,i}^{(3)} \qquad (21) \end{aligned}$$

The unit vectors $b_{R1}^{(1)}$, $b_{R1}^{(2)}$, and $b_{R1}^{(3)}$ have been introduced to allow a general rotor blade hinge sequence. For example, if rotor 1 blades undergo a lag, flap, and pitch rotation sequence, then $b_{R1}^{(1)} = \{0,0,1\}^T$, $b_{R1}^{(2)} = \{0,1,0\}^T$, and $b_{R1}^{(3)} = \{1,0,0\}^T$. Equation 21 has been obtained using the concept of simple angular velocities [7].

The body axis components of the fuselage c.g. velocity are given as,

$$v_B = \{u, v, w\}^T \tag{22}$$

The inertial axis components of the fuselage and blade c.g. velocities can be written as,

$$\begin{aligned} v_{F^\bullet} &= T_F v_B && (23)\\ v_{R1,i^\bullet} &= v_{F^\bullet} + \\ & T_F S(\omega_F)\bar{r}_{F1} + \\ & T_F T_{S1} S(\omega_{S1})\bar{r}_{H1} + \\ & T_F T_{S1} T_{H1,i} S(\omega_{H1,i})\bar{r}_{R1}^{(1)} + \\ & T_F T_{S1} T_{H1,i} T_{R1,i}^{(1)} S(\omega_{R1,i}^{(1)})\bar{r}_{R1}^{(2)} + \\ & T_F T_{S1} T_{H1,i} T_{R1,i}^{(1)} T_{R1,i}^{(2)} S(\omega_{R1,i}^{(2)})\bar{r}_{R1}^{(3)} + \\ & T_F T_{S1} T_{H1,i} T_{R1,i}^{(1)} T_{R1,i}^{(2)} T_{R1,i}^{(3)} S(\omega_{R1,i})\bar{r}_{R1}^{*} \\ & && (24) \end{aligned}$$

In Equation 24, ω_{S1} represents the body axis components of the angular velocity of rotor 1 shaft. $\omega_{H1,i}$, $\omega_{R1,i}^{(1)}$, and $\omega_{R1,i}^{(2)}$ are the individual body axis components of the angular velocities of the rotating hub, link 1, and link 2, respectively. The expressions for these angular velocities are given as follows:

$$\begin{aligned} \omega_{S1} &= [T_{S1}]^T \omega_F && (25)\\ \omega_{H1,i} &= [T_{H1,i}]^T \omega_{S1} + \{0, 0, -\Omega_{R1}\}^T && (26)\\ \omega_{R1,i}^{(1)} &= \left[T_{R1,i}^{(1)}\right]^T \omega_{H1,i} + b_{R1}^{(1)}\dot{\alpha}_{R1,i}^{(1)} && (27)\\ \omega_{R1,i}^{(2)} &= \left[T_{R1,i}^{(2)}\right]^T \omega_{R1,i}^{(1)} + b_{R1}^{(2)}\dot{\alpha}_{R1,i}^{(2)} && (28) \end{aligned}$$

In Equation 24, the vectors $\bar{r}_{F1}$, $\bar{r}_{H1}$, $\bar{r}_{R1}^{(1)}$, $\bar{r}_{R1}^{(2)}$, $\bar{r}_{R1}^{(3)}$, and $\bar{r}_{R1}^{*}$ are defined as follows. $\bar{r}_{F1}$ is the position vector from fuselage c.g. to a point on shaft 1, expressed in fuselage axes. $\bar{r}_{H1}$ is the position vector from the point on shaft 1 to the center of hub 1, expressed in shaft 1 axes. For any rotor 1 blade, $\bar{r}_{R1}^{(1)}$ is the position vector from the center of hub 1 to the first hinge, expressed in rotating hub 1 axes; $\bar{r}_{R1}^{(2)}$ is the position vector from the first hinge to the second hinge, expressed in link 1 axes; $\bar{r}_{R1}^{(3)}$ is the position vector from the second hinge to the third hinge, expressed in link 2 axes; and $\bar{r}_{R1}^{*}$ is the position vector from the third hinge to the blade c.g., expressed in blade axes. Equations 20 through 24 are used to compute the partial velocities and partial angular velocities needed in Equation 2.

The angular acceleration vectors $\dot{\omega}_F$ and $\dot{\omega}_{R1,i}$ appearing in Equation 2 are obtained by a time-differentiation of the right hand sides of Equations 20 and 21, respectively. Similarly, the translational acceleration vectors $a_{F^\bullet}$ and $a_{R1,i^\bullet}$ appearing in Equation 2 are obtained by a time-differentiation of the right hand sides of Equations 23 and 24, respectively. While the equations for the rotor blade acceleration vectors are lengthy and omitted here, it is noticed from an inspection of Equations 20 through 24 that obtaining these equations is straight forward once the expressions for the time-derivatives of the transformation matrices has been obtained. The Appendix gives the derivation of a formula for calculating the time-derivative of a matrix in terms of a matrix product. Using this formula, the following are obtained:

$$\begin{aligned} \dot{T}_F &= T_F S(\omega_F) && (29)\\ \dot{T}_{S1} &= 0 && (30)\\ \dot{T}_{H1,i} &= T_{H1,i} S\left(\{0, 0, -\Omega_{R1}\}^T\right) && (31)\\ \dot{T}_{R1,i}^{(1)} &= T_{R1,i}^{(1)} S\left(b_{R1}^{(1)}\dot{\alpha}_{R1,i}^{(1)}\right) && (32)\\ \dot{T}_{R1,i}^{(2)} &= T_{R1,i}^{(2)} S\left(b_{R1}^{(2)}\dot{\alpha}_{R1,i}^{(2)}\right) && (33)\\ \dot{T}_{R1,i}^{(3)} &= T_{R1,i}^{(3)} S\left(b_{R1}^{(3)}\dot{\alpha}_{R1,i}^{(3)}\right) && (34) \end{aligned}$$

Generalized Gravity Forces

The partial velocities $\frac{\partial v_{F^\bullet}}{\partial u_r}$, $\frac{\partial v_{R1,i^\bullet}}{\partial u_r}$, and $\frac{\partial v_{R2,i^\bullet}}{\partial u_r}$ obtained in the computation of generalized inertia forces are used to compute the generalized gravity forces given by Equation 3.

Generalized Aerodynamic Forces Due to Fuselage

The first term in Equation 4 represents the generalized aerodynamic forces due to the fuselage. The quantities comprising this term are obtained as follows. The body axis components of the velocity of the fuselage aerodynamic center (a.c.) can be written as,

$$v_F = v_B + S(\omega_F)\bar{r}_{AC} \tag{35}$$

where $\bar{r}_{AC}$ is the position vector from the fuselage c.g. to the fuselage a.c., expressed in body axes. Equation 35 is used to compute the partial velocity $\frac{\partial v_F}{\partial u_r}$.

For a rotorcraft, the wind-axis components of the aerodynamic force and moment acting at the fuselage a.c. are usually given as a function of fuselage angles of attack and sideslip:

$$\begin{aligned} L &= L_1(\alpha) + L_2(\beta) && (36)\\ D &= D_1(\alpha) + D_2(\beta) && (37)\\ M &= M_1(\alpha) + M_2(\beta) && (38) \end{aligned}$$

$$Y = Y_1(\alpha) + Y_2(\beta) \quad (39)$$
$$l = l_1(\alpha) + l_2(\beta) \quad (40)$$
$$N = N_1(\alpha) + N_2(\beta) \quad (41)$$

These forces and moments are scaled with respect to the local dynamic pressure and can be in the form of a two dimensional data table or fitted analytical expressions to wind-tunnel data. The force and moment components in the body axes are given as,

$$F_F = \bar{q}E_2(\alpha)E_3(-\beta)\{-D, Y, -L\}^T \quad (42)$$
$$M_F = \bar{q}E_2(\alpha)E_3(-\beta)\{l, M, N\}^T \quad (43)$$

The fuselage velocities, for purposes of calculating the aerodynamic variables α, β, and $\bar{q}$, include the effect of rotor 1 downwash:

$$\bar{v} = v_F - w_{R1,0} f_{R1}(\chi_{R1}) \quad (44)$$

where $w_{R1,0}$ is the rotor 1 collective inflow, and χ_{R1} is the rotor 1 wake skew angle. In absence of more sophisticated data, f_{R1} assumes the value $\{0,0,1\}^T$ or $\{0,0,0\}^T$, depending on whether the a.c. is within or outside of rotor 1 wake. χ_{R1} is given as,

$$\chi_{R1} = \tan^{-1}\left(\frac{\mu_{R1}}{-\lambda_{R1}}\right) \quad (45)$$

where μ_{R1} and λ_{R1} are, respectively, the rotor 1 advance ratio and rotor 1 inflow ratio. These quantities can be determined by computing the relative air velocity components at the rotor hub. Using Equation 44, the aerodynamic variables α, β, and $\bar{q}$ can be readily computed:

$$\alpha = \tan^{-1}\left(\frac{\bar{v}_3}{\bar{v}_1}\right), \quad \beta = \sin^{-1}\left(\frac{\bar{v}_2}{|\bar{v}|}\right) \quad (46)$$

$$\bar{q} = \frac{1}{2}\rho\,|\bar{v}|^2 \quad (47)$$

Generalized Aerodynamic Forces Due to Rotors

The second term in Equation 4 represents the generalized aerodynamic forces due to rotor 1. Blade element analysis is used to calculate this term. As mentioned earlier, the rotor blades are allowed to have any arbitrary variation of twist, chord length, and airfoil characteristics along the span. The body axis components of the blade element velocity are given as,

$$\begin{aligned} v_{R1,i,j} = {} & \left[T_F T_{S1} T_{H1,i} T^{(1)}_{R1,i} T^{(2)}_{R1,i} T^{(3)}_{R1,i}\right]^T v_{F^*} + \\ & \left[T_{S1} T_{H1,i} T^{(1)}_{R1,i} T^{(2)}_{R1,i} T^{(3)}_{R1,i}\right]^T S(\omega_F)\bar{r}_{F1} + \\ & \left[T_{H1,i} T^{(1)}_{R1,i} T^{(2)}_{R1,i} T^{(3)}_{R1,i}\right]^T S(\omega_{S1})\bar{r}_{H1} + \\ & \left[T^{(1)}_{R1,i} T^{(2)}_{R1,i} T^{(3)}_{R1,i}\right]^T S(\omega_{H1,i})\bar{r}^{(1)}_{R1} + \\ & \left[T^{(2)}_{R1,i} T^{(3)}_{R1,i}\right]^T S(\omega^{(1)}_{R1,i})\bar{r}^{(2)}_{R1} + \\ & \left[T^{(3)}_{R1,i}\right]^T S(\omega^{(2)}_{R1,i})\bar{r}^{(3)}_{R1} + \\ & S(\omega_{R1,i})\bar{r}_{R1,j} \end{aligned} \quad (48)$$

The only new quantity introduced in the preceding Equation is $\bar{r}_{R1,j}$ ($j = 1, \ldots, b_{R1}$), which is the position vector from the root of the blade to the jth aerodynamic element, expressed in blade body axes. Equation 48 is used to obtain the partial velocity $\frac{\partial v_{R1,i,j}}{\partial u_r}$.

Figure 3 shows a typical jth element on the ith blade, and the lift and drag forces acting on it. $(y_{R1,i}, z_{R1,i})$ are the body axes of the blade. $\theta_{R1,j}$ is the blade twist angle at the jth section. $u^s_{R1,i,j}$ and $u^p_{R1,i,j}$ are the components of the relative air velocity parallel and perpendicular to the zero lift line. The variables $\alpha_{R1,i,j}$, $L_{R1,i,j}$, and $D_{R1,i,j}$ have obvious meanings. The velocity of the (i,j)th element with respect to air is given by the following equation,

$$\bar{v}_{R1,i,j} = v_{R1,i,j} + \left[T_{H1,i} T^{(1)}_{R1,i} T^{(2)}_{R1,i} T^{(3)}_{R1,i}\right]^T v^A_{R1,i,j} \quad (49)$$

The term $v^A_{R1,i,j}$ arises due to rotor inflow and can be approximately evaluated as,

$$\begin{aligned} (v^A_{R1,i,j})_1 &= 0 \\ (v^A_{R1,i,j})_2 &= 0 \\ (v^A_{R1,i,j})_3 &= -w_{R1,0} - [h_{R1} + (\bar{r}_{R1,j})_1/R_{R1}]\cdot \\ & \quad (w_{R1,1s}\sin\psi_{R1,i} + w_{R1,1c}\cos\psi_{R1,i}) \end{aligned} \quad (50)$$

where

$$h_{R1} = \frac{(\bar{r}^{(1)}_{R1})_1 + (\bar{r}^{(2)}_{R1})_1 + (\bar{r}^{(3)}_{R1})_1}{R_{R1}} \quad (51)$$

$w_{R1,1s}$ and $w_{R1,1c}$ are the sin and cos components of the rotor inflow and R_{R1} is the rotor radius. The radial, tangential, and perpendicular components of the air velocity at the airfoil can be computed as,

$$\{u^r_{R1,i,j}, -u^s_{R1,i,j}, u^p_{R1,i,j}\}^T = E_1(\theta_{R1,j})\bar{v}_{R1,i,j} \quad (52)$$

Using the air velocity components, the section angle of attack and Mach Number can be calculated as follows:

$$\alpha_{R1,i,j} = \tan^{-1}\left(\frac{u^p_{R1,i,j}}{u^s_{R1,i,j}}\right) \quad (53)$$

$$\mathcal{M}_{R1,i,j} = \frac{\sqrt{(u^s_{R1,i,j})^2 + (u^p_{R1,i,j})^2}}{c} \quad (54)$$

where c is the speed of sound at the altitude where the aircraft is operating. Airfoil lift and drag coefficients are usually specified as a function of the angle of attack and Mach Number. Thus,

$$c^l_{R1,i,j} = c^l_{R1,i,j}(\alpha_{R1,i,j}, \mathcal{M}_{R1,i,j}) \quad (55)$$

$$c^d_{R1,i,j} = c^d_{R1,i,j}(\alpha_{R1,i,j}, \mathcal{M}_{R1,i,j}) \quad (56)$$

The above data can be either in the form of a two dimensional data table or in the form of fitted analytical expressions to experimental data. However, in the absence of any data, simple analytical lift and drag models can be used. Based on reference [9], equations were generated for two simple models, one that ignored stall and compressibility effects and another that included the same. The section lift and drag forces are computed next:

$$\begin{aligned} L_{R1,i,j} &= \bar{q}_{R1,i,j} c^l_{R1,i,j} c_{R1,j} (\Delta \bar{r}_{R1,j})_1 \eta_{R1,j} \quad (57) \\ D_{R1,i,j} &= \bar{q}_{R1,i,j} c^d_{R1,i,j} c_{R1,j} (\Delta \bar{r}_{R1,j})_1 \quad (58) \end{aligned}$$

where

$$\bar{q}_{R1,i,j} = \frac{1}{2}\rho[(u^s_{R1,i,j})^2 + (u^p_{R1,i,j})^2] \quad (59)$$

and $c_{R1,j}$ and $\eta_{R1,j}$ are, respectively, the chord length and lift efficiency factors at the jth section. The body axis components of the section aerodynamic force are given by:

$$F_{R1,i,j} = E_1(\alpha_{R1,i,j} - \theta_{R1,j})\{0, D_{R1,i,j}, -L_{R1,i,j}\}^T \quad (60)$$

Generalized Aerodynamic Forces Due to Surfaces

The generalized aerodynamic forces due to the external surfaces are derived in much the same way as those due to the rotors. One difference, however, is that the radial drag force due to radial flow is considered here. It is assumed that every surface has a fixed (invariant with time) orientation with respect to the fuselage. The orientation can be specified uniquely in terms of rotation angles about three mutually perpendicular axes. In order to have consistency in describing surfaces with different orientations, the body axes for any surface are defined as follows. The x axis coincides with the zero lift line of the root section and is directed from the trailing edge of the surface to the leading edge of the surface (see Figure 4). The y axis is perpendicular to the x axis, passes through the aerodynamic center of the root section and is directed outboard. z axis completes the right handed set.

The objective is to evaluate the last term in Equation 4. For illustration purposes, the mathematical analysis involved is outlined for surface 1. Let the surface be oriented with respect to the fuselage by three successive rotations of angles γ_{S_1}, δ_{S_1} and ϵ_{S_1} about mutually perpendicular axes. The sequence of rotations can be any of the possible six sequences. Let the matrices associated with the above transformations be $T^{(1)}_{S_1}$, $T^{(2)}_{S_1}$, and $T^{(3)}_{S_1}$, respectively. The matrix $T_{ES_1} = T^{(3)}_{S_1}(\epsilon_{S_1})T^{(2)}_{S_1}(\delta_{S_1})T^{(1)}_{S_1}(\gamma_{S_1})$ transforms components of a vector from fuselage axes to surface 1 axes. Let $\bar{r}_{S_1}$ be the position vector from the fuselage c.g. to the surface 1 reference point, expressed in fuselage axes. Let $\bar{r}_{S_1,j}$ be the position vector from the surface reference point to the aerodynamic center of the jth section, expressed in surface axes. Then the velocity of the jth section can be expressed as,

$$v_{S_1,j} = T_{ES_1}\left[v_B + S(\omega_F)\bar{r}_{S_1} + S(\omega_F)[T_{ES_1}]^T \bar{r}_{S_1,j}\right] \quad (61)$$

This expression is used to obtain the partial velocity $\frac{\partial v_{S_1,j}}{\partial u_r}$, which is needed for evaluating the generalized aerodynamic force contribution from surface 1.

For purposes of computing the aerodynamic force, the resultant section velocity with respect to air includes the effect of rotor 1 downwash:

$$\bar{v}_{S_1,j} = v_{S_1,j} - T_{ES_1} w_{R1,0} f_{S_1}(\chi_{R1}) \quad (62)$$

Similar to the case of the fuselage, in a simple analysis, f_{S_1} can be taken to be equal to $\{0,0,1\}^T$ or $\{0,0,0\}^T$, depending on whether the surface is within or outside of rotor 1 wake.

The effect of radial flow on a surface section is included in the same way as described in reference [10], where profile power is computed due to radial flow at blade sections. Let the free stream velocity at the jth section be yawed, as shown in Figure 5. An estimate of the normal and radial drag forces is desired, preferably in terms of the two dimensional sectional aerodynamic coefficients. It is assumed that the total viscous drag on the yawed section acts in the same direction as the free stream velocity. It is also assumed that the yawed section drag coefficient is given by the two dimensional unyawed airfoil characteristics. The normal section lift coefficient is assumed not to be influenced by yawed flow. The angle of attack and Mach Number for the unyawed and yawed sections are,

$$\begin{aligned} \alpha_{S_1,j} &= \tan^{-1}\left(\frac{(\bar{v}_{S_1,j})_3}{(\bar{v}_{S_1,j})_1}\right) \quad (63) \\ \mathcal{M}_{S_1,j} &= \frac{\sqrt{(\bar{v}_{S_1,j})_1^2 + (\bar{v}_{S_1,j})_3^2}}{c} \quad (64) \\ \hat{\alpha}_{S_1,j} &= \tan^{-1}\left(\frac{(\bar{v}_{S_1,j})_3}{\sqrt{(\bar{v}_{S_1,j})_1^2 + (\bar{v}_{S_1,j})_2^2}}\right) \quad (65) \end{aligned}$$

$$\hat{\mathcal{M}}_{S_1,j} = \frac{\sqrt{(\bar{v}_{S_1,j})_1^2 + (\bar{v}_{S_1,j})_2^2 + (\bar{v}_{S_1,j})_3^2}}{c} \quad (66)$$

The section lift and drag coefficients are given by:

$$c^l_{S_1,j} = c^l_{S_1,j}(\alpha_{S_1,j}, \mathcal{M}_{S_1,j}) \quad (67)$$

$$c^d_{S_1,j} = c^d_{S_1,j}(\hat{\alpha}_{S_1,j}, \hat{\mathcal{M}}_{S_1,j}) \quad (68)$$

As mentioned for the case of rotor aerodynamics, in the absence of lift and drag coefficient data, simple analytical models for the coefficients can be used. The section lift and drag forces are given as,

$$\begin{aligned} L_{S_1,j} &= \bar{q}_{S_1,j} c^l_{S_1,j} c_{S_1,j} (\Delta \bar{r}_{S_1,j})_2 \eta_{S_1,j} && (69) \\ D_{S_1,j} &= \hat{q}_{S_1,j} c^d_{S_1,j} c_{S_1,j} (\Delta \bar{r}_{S_1,j})_2 && (70) \end{aligned}$$

where

$$\begin{aligned} \bar{q}_{S_1,j} &= \frac{1}{2}\rho[(\bar{v}_{S_1,j})_1^2 + (\bar{v}_{S_1,j})_3^2] && (71) \\ \hat{q}_{S_1,j} &= \frac{1}{2}\rho[(\bar{v}_{S_1,j})_1^2 + (\bar{v}_{S_1,j})_2^2 + (\bar{v}_{S_1,j})_3^2] && (72) \end{aligned}$$

and $\eta_{S_1,j}$ is the section lift efficiency factor. Finally, the body axis components of the section aerodynamic force are given as,

$$\begin{aligned} R_{S_1,j} = & \left(L_{S_1,j} / \sqrt{(\bar{v}_{S_1,j})_1^2 + (\bar{v}_{S_1,j})_3^2} \right) \cdot \\ & \{(\bar{v}_{S_1,j})_3, 0, -(\bar{v}_{S_1,j})_1\}^T + \\ & \left(D_{S_1,j} / \sqrt{(\bar{v}_{S_1,j})_1^2 + (\bar{v}_{S_1,j})_2^2 + (\bar{v}_{S_1,j})_3^2} \right) \cdot \\ & \{-(\bar{v}_{S_1,j})_1, -(\bar{v}_{S_1,j})_2, -(\bar{v}_{S_1,j})_3\}^T \quad (73) \end{aligned}$$

Generalized Damping Forces Due to Translational Dampers

As shown in Figure 2, one end of the blade translational damper is attached to the rotating hub while the other end is attached to the blade itself. The damper force is assumed to be given as a function of the relative speed between it's two ends. The analysis associated with the first term in Equation 5, which is due to rotor 1, is developed in the following. The position vector from attachment point 1 to attachment point 2, expressed in the rotating hub axes, is given as,

$$\begin{aligned} d_{R1,i} = & \left(\bar{r}^{(1)}_{R1} - \bar{s}_{R1} \right) + \\ & T^{(1)}_{R1,i} \bar{r}^{(2)}_{R1} + \\ & T^{(1)}_{R1,i} T^{(2)}_{R1,i} \bar{r}^{(3)}_{R1} + \\ & T^{(1)}_{R1,i} T^{(2)}_{R1,i} T^{(3)}_{R1,i} \bar{t}_{R1} \quad (74) \end{aligned}$$

$\bar{s}_{R1}$ is the position vector from the center of the hub to attachment point 1, expressed in hub axes. $\bar{t}_{R1}$ is the position vector from the blade root to attachment point 2, expressed in blade axes. The preceding equation is used to determine the velocity of attachment point 2 relative to that of attachment point 1, expressed in hub axes:

$$\begin{aligned} \tilde{v}_{R1,i} = & S(\omega_{H1,i}) \left(\bar{r}^{(1)}_{R1} - \bar{s}_{R1} \right) + \\ & T^{(1)}_{R1,i} S(\omega^{(1)}_{R1,i}) \bar{r}^{(2)}_{R1} + \\ & T^{(1)}_{R1,i} T^{(2)}_{R1,i} S(\omega^{(2)}_{R1,i}) \bar{r}^{(3)}_{R1} + \\ & T^{(1)}_{R1,i} T^{(2)}_{R1,i} T^{(3)}_{R1,i} S(\omega_{R1,i}) \bar{t}_{R1} \quad (75) \end{aligned}$$

The component of this relative velocity along the damper arm can be written as,

$$\hat{v}_{R1,i} = (1/\mid d_{R1,i} \mid)(d_{R1,i})^T \tilde{v}_{R1,i} \quad (76)$$

The damper force $F_{R1,i}$ is assumed to be specified as a function of the above speed. Hence,

$$F_{R1,i} = F_{R1,i}(\hat{v}_{R1,i}) \quad (77)$$

The hub axis components of the forces acting at the attachment points are given as,

$$\begin{aligned} F^D_{R1,i,1} &= -(F_{R1,i}/\mid d_{R1,i} \mid) d_{R1,i} && (78) \\ F^D_{R1,i,2} &= (F_{R1,i}/\mid d_{R1,i} \mid) d_{R1,i} && (79) \end{aligned}$$

The velocities at the attachment points, expressed in the hub axes, are:

$$\begin{aligned} v^D_{R1,i,1} = & [T_{S1} T_{H1,i}]^T (v_B + S(\omega_F) \bar{r}_{F1}) + \\ & [T_{H1,i}]^T S(\omega_{S1}) \bar{r}_{H1} + \\ & S(\omega_{H1,i}) \bar{s}_{R1} \quad (80) \\ v^D_{R1,i,2} = & v^D_{R1,i,1} + \tilde{v}_{R1,i} \quad (81) \end{aligned}$$

The above two equations are used to calculate the required partial velocities, $\frac{\partial v^D_{R1,i,1}}{\partial u_r}$ and $\frac{\partial v^D_{R1,i,2}}{\partial u_r}$.

Generalized Spring-Damper Forces Due to Torsional Spring-Dampers

The torsional springs and dampers mounted on the blade hinges are assumed to possess linear stiffness and damping properties. They give rise to the third and fourth terms in Equation 5. The third term in this equation is due to rotor 1 and is discussed below. Referring to Figure 2, the following quantities are defined for the ith blade. $M_{R1,i,1}$ denotes the body axis components of the moment on acting link 1 due to the spring-damper at hinge 1. $M_{R1,i,2}$ denotes the body axis components of the moment on acting link 2 due to the spring-damper at hinge 2. $M_{R1,i,3}$ denotes the body axis components of the moment on acting on the blade due to the spring-damper at hinge 3. These moments can be expressed as,

$$M_{R1,i,1} = -b_{R1}^{(1)}\left(k_{P_{R1}}^{(1)}\alpha_{R1,i}^{(1)} + k_{D_{R1}}^{(1)}\dot{\alpha}_{R1,i}^{(1)}\right) \quad (82)$$

$$M_{R1,i,2} = -b_{R1}^{(2)}\left(k_{P_{R1}}^{(2)}\alpha_{R1,i}^{(2)} + k_{D_{R1}}^{(2)}\dot{\alpha}_{R1,i}^{(2)}\right) \quad (83)$$

$$M_{R1,i,3} = -b_{R1}^{(3)}\left(k_{P_{R1}}^{(3)}\alpha_{R1,i}^{(3)} + k_{D_{R1}}^{(3)}\dot{\alpha}_{R1,i}^{(3)}\right) \quad (84)$$

where k_P and k_D denote sttifness and damping constants. The torsional spring-damper moments acting on the hub, link 1, link 2, and the blade, expressed in their individual body axes, are respectively given as,

$$M_{R1,i,1}^{D} = -M_{R1,i,1} \quad (85)$$

$$M_{R1,i,2}^{D} = M_{R1,i,1} - M_{R1,i,2} \quad (86)$$

$$M_{R1,i,3}^{D} = M_{R1,i,2} - M_{R1,i,3} \quad (87)$$

$$M_{R1,i,4}^{D} = M_{R1,i,3} \quad (88)$$

The individual body axis components of the angular velocities of the hub, link 1, link 2, and the blade, are respectively given as,

$$\omega_{R1,i,1}^{D} = \omega_{H1,i} \quad (89)$$

$$\omega_{R1,i,2}^{D} = \omega_{R1,i}^{(1)} \quad (90)$$

$$\omega_{R1,i,3}^{D} = \omega_{R1,i}^{(2)} \quad (91)$$

$$\omega_{R1,i,4}^{D} = \omega_{R1,i} \quad (92)$$

The preceding four equations are used to compute the four partial velocities needed for evaluating the third term in Equation 5.

Airframe Kinematics

To complete the description of the airframe dynamic model, the kinematic relationship between the vectors q, $\dot{q}$, and u needs to be stipulated. Let the airframe kinematic equations be given as,

$$f_{K_i}(q, \dot{q}, u) = 0, \quad i = 1, \ldots, n_{RB} \quad (93)$$

The elements of the vector f_{K_i} are given in detail as follows:

$$\left\{ \begin{array}{c} f_{K_1} \\ \vdots \\ f_{K_6} \end{array} \right\} = u_F - \left[\begin{array}{cc} [T_F]^T & 0 \\ 0 & W_B \end{array} \right] \dot{q}_F \quad (94)$$

$$\left\{ \begin{array}{c} f_{K_7} \\ \vdots \\ \vdots \\ f_{K_{n_{RB}}} \end{array} \right\} = \left\{ \begin{array}{c} u_{R1,1} \\ \vdots \\ u_{R1,n_{R1}} \\ u_{R2,1} \\ \vdots \\ u_{R2,n_{R2}} \end{array} \right\} - \left\{ \begin{array}{c} \dot{q}_{R1,1} \\ \vdots \\ \dot{q}_{R1,n_{R1}} \\ \dot{q}_{R2,1} \\ \vdots \\ \dot{q}_{R2,n_{R2}} \end{array} \right\} \quad (95)$$

The matrix W_B is given as,

$$W_B = \left[\begin{array}{ccc} 1 & 0 & -\sin\theta \\ 0 & \cos\phi & \sin\phi\cos\theta \\ 0 & -\sin\phi & \cos\phi\cos\theta \end{array} \right] \quad (96)$$

Multiblade Coordinate Transformation

The airframe dynamic and kinematic models, given by Equations 1 and 93, respectively, are derived in the rotating system, with the rotor degrees of freedom describing the motion of individual rotor blades. However, the rotor usually responds as a whole to excitation and for physical insight it is desirable to work with the degrees of freedom which model the entire rotor system rather than the individual blades. To transform the equations of motion with respect to individual blade coordinates to rotor system coordinates, the method of multiblade coordinates is used [11]. Considering the example of rotor 1, for like degrees of freedom, the kth ($k = 1, \ldots, n_{R1}$) individual rotor blade degree of freedom is expressed as,

$$\alpha_{R1,k} = \alpha_{R1,0} + \sum_{i=1}^{(n_{R1}-1)/2} (\alpha_{R1,ic}\cos i\psi_k + \alpha_{R1,is}\sin i\psi_k) \quad (97)$$

for rotors with an odd number of blades and

$$\alpha_{R1,k} = \alpha_{R1,0} + \sum_{i=1}^{(n_{R1}-2)/2} (\alpha_{R1,ic}\cos i\psi_k + \alpha_{R1,is}\sin i\psi_k) + \alpha_{R1,d}(-1)^k \quad (98)$$

for rotors with an even number of rotor blades.

Let the generalized coordinate and generalized speed vectors in the multiblade or non-rotating coordinate system be represented by q' and u'. Then the following substitutions are made in the airframe kinematic and dynamic model descriptions, given by Equations 93 and 1, respectively.

$$q = T(t)q' \quad (99)$$

$$u = \dot{T}(t)q' + T(t)u' \quad (100)$$

$$\dot{u} = \ddot{T}(t)q' + 2\dot{T}(t)u' + T(t)\dot{u}' \quad (101)$$

Then the resulting airframe kinematic and dynamic equations can be written as,

$$f_{K_i}(q', \dot{q}', u') = 0, \quad i = 1, \ldots, n_{RB} \quad (102)$$

$$f_i(q', u', w, \dot{u}', t) = 0, \quad i = 1, \ldots, n_{RB} \quad (103)$$

where the vector w consists of the inflow coordinates of the two rotors:

$$w = \{w_{R1,0}, w_{R1,1s}, w_{R1,1c}, w_{R2,0}, w_{R2,1s}, w_{R2,1c}\}^T \tag{104}$$

Rotor Dynamic Inflow Model

The rotor dynamic inflow model used in this work is based on the Peters and HaQuang [12] model which is in turn based on the work of Pitt and Peters [8]. The model includes three inflow degrees of freedom that yield the time-varying induced flow parallel to the rotor shaft. Based on the small perturbation potential flow equations, the model accounts for dynamic changes in collective inflow and first harmonic inflow azimuthally. Inflow along the blades varies linearly. The inflow distribution is given by Equation 50. For simplicity only the dynamic inflow model for rotor 1 will be described. The dynamic inflow model for rotor 2 is similar with obvious changes.

The basic model formulation is carried out in the rotor wind axis system and is later transformed to the rotor shaft axis system. The dynamic inflow equations are forced by the averaged (over rotor revolution) rotor thrust, rolling moment, and pitching moment in the shaft axes. The resulting equations can be written in the form,

$$\left\{ \begin{array}{c} \dot{w}_{R1,0} \\ w_{R1,1s} \\ w_{R1,1c} \end{array} \right\} + [\mathcal{A}_{R1}] \left\{ \begin{array}{c} w_{R1,0} \\ w_{R1,1s} \\ w_{R1,1c} \end{array} \right\} = \left\{ \begin{array}{c} \frac{-\bar{T}_{R1}}{\rho\pi R_1^3} \\ \frac{-\bar{L}_{R1}}{\rho\pi R_1^4} \\ \frac{\bar{M}_{R1}}{\rho\pi R_1^4} \end{array} \right\} \tag{105}$$

where,

$$\mathcal{A}_{R1} = \mathcal{A}_{R1}(q', u') \tag{106}$$

The blade element forces, given by Equation 60, are vectorially summed over all rotor blades to obtain the shaft axis components of the rotor thrust, rolling moment and pitching moment. These forces and moments are then averaged over the period of revolution of the rotor and used in Equation 105.

The complete set of dynamic inflow equations for the two rotors can be functionally represented as,

$$g_i(q', u', w, \dot{w}) = 0, \quad i = 1, \ldots, n_{DI} \tag{107}$$

where $n_{DI} = 6$ since three state inflow models are being used for each rotor. It should be noted that Equation 107 is written using the multiblade or non-rotating coordinate system.

Trim Algorithm

Trim of an aircraft is defined as an equilibrium condition where the translational and rotational accelerations of the fuselage are zero. Hence in trim, $\dot{p} = \dot{q} = \dot{r} = \dot{u} = \dot{v} = \dot{w} = 0$. For straight and level flight, $p = q = r = v = 0$ as well. For a fixed wing airplane this definition is sufficient since one can generally regard an airplane as a single rigid body with six degrees of freedom. For rotorcraft the concept of trim is more complicated because the vehicle is represented as a multibody system consisting of a fuselage, many rotor blades, and a drive system. By virtue of the rotor rotational motion, the blades are always accelerating. For the rotor blade degrees of freedom, trim is considered to be an operating condition such that the individual rotor blades follow a periodic path. This implies that all the first and second derivatives of the rotor multiblade coordinates must be zero in trim. This will force individual blades to track the same periodic path each rotor revolution. However, it should be noted that for even bladed rotors this condition will not force every blade on a rotor to follow the same path. This is due to the warping multiblade coordinate mode for even bladed rotors.

There are many different methods for obtaining the trim condition of a coupled rotor and fuselage combination. Included in these methods are iterative fuselage trim and rotor trim, fully coupled autopilot trim, finite elements in time trim, nonlinear optimization trim, and Galerkin method trim. While no one method for trim is superior in all settings, all the methods are sufficiently different to have qualities which make them more or less attractive in different settings. In this work a nonlinear optimization trim technique is used.

In nonlinear optimization, one seeks to minimize or maximize a certain nonlinear function by iterating on the independent variables of the problem. Here the sum of the squares of the dynamic equation residuals will be minimized and the independent variables will be the system states and controls. A modified Newton's method, sometimes called a damped Newton's method or a quasi Newton method, is used as the nonlinear optimization algorithm to compute the trim state of the vehicle.

The trim algorithm begins by noting that in trim, $\dot{u}' = 0$ and $\dot{w} = 0$ necessarily. Hence in trim, the airframe dynamic equations (Equation 1) and the dynamic inflow equations (Equation 107) can be written as,

$$\begin{aligned} f_i(x, t) &= 0, \quad i = 1, \ldots, n_{RB} && (108) \\ g_i(x) &= 0, \quad i = 1, \ldots, n_{DI} && (109) \end{aligned}$$

where

$$x = \{(q')^T, (u')^T, (w)^T\}^T \tag{110}$$

Clearly, x is the state vector of the airframe dynamic model. Equation 108 contains a set of algebraic nonlinear equations which are periodic in time, with a period of τ. τ is the period of revolution common to rotor 1 blades and rotor 2 blades. The goal of the trim algorithm is to minimize the residual of each equation in Equations 108 and 109 for all values of time.

A natural scalar function to minimize for trim is,

$$\begin{aligned} J &= \frac{1}{\tau}\int_0^{\tau}\sum_{i=1}^{n_{RB}} f_i(t)^2 dt + \sum_{i=1}^{n_{DI}} g_i^2 \\ &\approx \frac{\Delta t}{\tau}\sum_{k=1}^{n_T}\sum_{i=1}^{n_{RB}} f_i(t_k)^2 + \sum_{i=1}^{n_{DI}} g_i^2 \end{aligned} \tag{111}$$

where n_T is the number of time points chosen for discretization. The function J is termed the cost function. Using the discretized form of the cost function, the gradient and hessian of the cost function can be formed.

$$\frac{\partial J}{\partial x_j} = 2\frac{\Delta t}{\tau}\sum_{k=1}^{n_T}\sum_{i=1}^{n_{RB}} f_i(t_k)\frac{\partial f_i(t_k)}{\partial x_j} + 2\sum_{i=1}^{n_{DI}} g_i \frac{\partial g_i}{\partial x_j} \tag{112}$$

$$\begin{aligned} &\frac{\partial}{\partial x_l}\left(\frac{\partial J}{\partial x_j}\right) \approx \\ &2\frac{\Delta t}{\tau}\sum_{k=1}^{n_T}\sum_{i=1}^{n_{RB}}\left[\frac{\partial f_i(t_k)}{\partial x_l}\frac{\partial f_i(t_k)}{\partial x_j} + f_i(t_k)\frac{\partial^2 f_i(t_k)}{\partial x_l \partial x_j}\right] \\ &+ 2\sum_{i=1}^{n_{DI}}\left[\frac{\partial g_i}{\partial x_l}\frac{\partial g_i}{\partial x_j} + g_i\frac{\partial^2 g_i}{\partial x_l \partial x_j}\right] \end{aligned} \tag{113}$$

The minimization problem described above is essentially a least squares problem. It is known that for least square minimization problems, where the cost function is small at the solution, the second derivative terms in the above equations are relatively small and can be neglected [13]. By definition, this assumption is valid in the trim problem.

In a modified Newton's method, a local optimization problem is solved iteratively. A flow chart for the iteration procedure is given in Figure 6. Using an initial condition or guess for the trim variables, a local quadratic model of the cost function is formed,

$$J(x+\Delta x) = J(x) + \frac{\partial J}{\partial x}\Delta x + \frac{1}{2}\Delta x^T \frac{\partial^2 J}{\partial x^2}\Delta x \tag{114}$$

At the local minimum of this approximation to the actual cost function one must have,

$$\frac{\partial J}{\partial \Delta x} = 0 \tag{115}$$

For a local minimum of a quadratic function to exist, hessian matrix of the cost function must be positive definite. Assuming this is the case,

$$\Delta x = -\left[\frac{\partial^2 J}{\partial x^2}\right]^{-1}\left\{\frac{\partial J}{\partial x}\right\} \tag{116}$$

The vector Δx is called the search direction because based on this direction a search to reduce the cost function shall be undertaken. For the local quadratic model of the cost function, the minimum is given by $x+\Delta x$, of course if a minimum exists. A new iteration on the minimum of the actual cost function can now be made by with the equation,

$$x_{new} = x_{old} + \alpha \Delta x \tag{117}$$

The parameter, α, is the step length. It is used because the local model is only an approximation to the actual cost. $\alpha = 1$ corresponds to a full Newton's method while $\alpha < 1$ implies a damped or modified Newton's method. The parameter α is determined at each trim iteration and is based on satisfying criteria for tracking sufficient decrease in the cost function at each iteration in the overall minimization problem. The process of determining the step length is called a step length procedure or line search strategy.

There are many criteria for determining sufficient decrease in the cost function at each iteration. Armijo's rule is used here which can be stated as,

$$J_0 - J_\alpha \geq -\mu\alpha\frac{\partial J}{\partial x}\Delta x \tag{118}$$

where the constant μ is a positive number. A back tracking strategy is used in the line search strategy. In this method, one always starts with $\alpha = 1$ and tries to use the full Newton's method if possible. If the current α does not fulfill the Armijo condition, then α is divided by a factor and retried. Once an appropriate value for α is obtained, new values for x are computed. Then a new local quadratic model is formed and the optimization procedure is again formed. It should be noted that in solving for the search direction a linear system must be solved. It is solved using a modified Choleski decomposition algorithm as described in reference [13].

Linear Model of Airframe Dynamics

Linearized rotorcraft dynamic models are extremely useful for flying qualities analyses. To this end, the composite airframe dynamic model consisting of the kinematic, dynamic, and dynamic inflow models, given by Equations 102, 103, and 107, respectively, is linearized about an arbitrary trim state, x_0. The linear model can be written as,

$$C_p(x_0,t)\delta\dot{x} = D_p(x_0,t)\delta x \tag{119}$$

The $(2n_{RB}+n_{DI}) \times (2n_{RB}+n_{DI})$ square matrices C_p and D_p are given as,

$$C_P = \begin{bmatrix} \frac{\partial f_K}{\partial \dot{q}'} & 0 & 0 \\ 0 & \frac{\partial f}{\partial \dot{u}'} & 0 \\ 0 & 0 & \frac{\partial g}{\partial \dot{w}} \end{bmatrix} \tag{120}$$

$$D_p = -\begin{bmatrix} \frac{\partial f_K}{\partial q'} & \frac{\partial f_K}{\partial u'} & 0 \\ \frac{\partial f}{\partial q'} & \frac{\partial f}{\partial u'} & \frac{\partial f}{\partial w} \\ \frac{\partial g}{\partial q'} & \frac{\partial g}{\partial u'} & \frac{\partial g}{\partial w} \end{bmatrix} \tag{121}$$

where

$$\begin{aligned} f_K &= \{f_{K_1},\ldots,f_{K_{n_{RB}}}\}^T & (122)\\ f &= \{f_1,\ldots,f_{n_{RB}}\}^T & (123)\\ g &= \{g_1,\ldots,g_{n_{DI}}\}^T & (124) \end{aligned}$$

In the ensuing analysis, the δ's in Equation 119 will be dropped and the perturbation state of the aircraft will be simply denoted as x_{ac}.

Transformation of the Airframe Linear Dynamic Equations

The multiblade coordinate transformation should be accompanied by a transformation of the equations of motion to the non-rotating coordinate system. This step is accomplished by taking linear combinations of the equations of motion given by Equation 119. The operations can be performed by premultiplying the dynamic equations by a transformation matrix, $\bar{T}(t)$. The fully transformed linear equations are,

$$\bar{T}(t)C_p(t)\dot{x}_{ac} = \bar{T}(t)D_p(t)x_{ac} \tag{125}$$

In rotorcraft handling qualities analysis, a linear time invariant system is most convenient to work with due to the powerful linear system analysis tools available. A standard approximation used in rotorcraft handling qualities work is to neglect the harmonic content in Equation 125 and hence obtain a linear time invariant system. This approximation is known as the constant coefficient approximation and it is used in the current effort.

The blade pitch control terms can be separated from the above equations by assuming that the multiblade coordinate blade pitch degrees of freedom do not possess dynamics. Appropriate rows of the dynamics matrix are deleted and the associated columns form the controls matrix. The final form of the airframe linear dynamic equations is,

$$\begin{aligned} \dot{x}_{ac} &= Ax_{ac} + B\vartheta & (126)\\ y_{ac} &= Cx_{ac} + D\vartheta & (127) \end{aligned}$$

where the vector ϑ consists of individual rotor pitch control variables. This system can now be coupled to the flight control system to form the complete system.

Linear Control System Model

Most aircraft flight control systems are given in block diagram form and there is no standard structure. Although for modeling purposes, a generic flight control system structure could be assumed such that all or at least a majority of current aircraft flight control systems could be accommodated, it is felt this approach may be too restrictive in some cases and far too general, hence inefficient, in other cases. It is desirable to have a flight control system modeling capability which does not assume a structure aprior but uses the input data deck to generate the model. This approach allows for greater flexibility and increased utility of the control system model. With these considerations in mind, a linear state-space flight control system modeling capability was developed that takes the basic block diagram data as input.

The flight control system is assumed to be comprised of an arbitrary number of filters, given in polynomial form. Each filter is a multi input and single output filter as shown in Figure 7.

The inputs to each filter can consist of pilot stick inputs, outputs of other individual filters, aircraft states, and derivatives of aircraft states. A state-space realization is computed for each individual filter in phase variable canonical form. The filters are then assembled into an overll state-space realization. The realization can be written as,

$$\dot{x}_{cs} = A_u x_{cs} + B_u v_u \tag{128}$$

$$y_u = C_u x_{cs} + D_u v_u \tag{129}$$

The subscript u signifies that the state-space matrices do not account for the filter coupling. A filter coupling matrix can be computed in the form,

$$v_u = \zeta_u y_u + \beta_u \delta + \gamma_u x_{ac} + \sigma_u \dot{x}_{ac} \tag{130}$$

It should be noted that Equations 128, 129 and 130 can be constructed in a straight forward manner from the input block diagram data. Substituting Equation

130 into Equations 128 and 129, the coupled state-space model of the control system can be formed.

$$\dot{x}_{cs} = F x_{cs} + G\delta + H x_{ac} + E\dot{x}_{ac} \quad (131)$$
$$\vartheta = P x_{cs} + Q\delta + R x_{ac} + Z\dot{x}_{ac} \quad (132)$$

where,

$$F = A_u + B_u\zeta_u S_u \quad (133)$$
$$G = B_u\zeta_u U_u + B_u\beta_u \quad (134)$$
$$H = B_u\zeta_u V_u + B_u\gamma_u \quad (135)$$
$$E = B_u\zeta_u W_u + B_u\sigma_u \quad (136)$$
$$P = X[C_u + D_u\zeta_u S_u] \quad (137)$$
$$Q = X[D_u\zeta_u U_u + D_u\beta_u] \quad (138)$$
$$R = X[D_u\zeta_u V_u + D_u\gamma_u] \quad (139)$$
$$Z = X[D_u\zeta_u W_u + D_u\sigma_u] \quad (140)$$
$$S_u = [I - D_u\zeta_u]^{-1} C_u \quad (141)$$
$$U_u = [I - D_u\zeta_u]^{-1} D_u\beta_u \quad (142)$$
$$V_u = [I - D_u\zeta_u]^{-1} D_u\gamma_u \quad (143)$$
$$W_u = [I - D_u\zeta_u]^{-1} D_u\sigma_u \quad (144)$$

The matrix X restricts the overall control system outputs to be the aircraft blade pitch angles. It should be noted that if the matrix $[I - D_u\zeta_u]$ is singular, then there is not a valid state-space model for the system and the system is non-causal. This is due to the fact that the flight control system output can be written as,

$$[I - D_u\zeta_u]\, y = C_u x_{cs} + D_u\beta_u\delta + D_u\gamma_u x_{ac} + D_u\sigma_u\dot{x}_{ac} \quad (145)$$

For a valid state-space realization the output must be uniquely determined from the state and control. Clearly when $[I - D_u\zeta_u]$ is singular this is not possible. This observation can be used for detecting input data errors.

Airframe and Control System Coupling

The linear airframe model which describes the rigid body aircraft motion and rotor dynamic inflow is given by Equations 126 and 127. The inputs to the airframe linear equations are blade pitch angles of the two rotor systems. The linear flight control system model is given by Equations 131 and 132. The outputs of the flight control system model are also the blade pitch angles of the two rotors. The linear airframe and control system models are coupled by noting that the output of the flight control system model is the input to the airframe model.

$$\left\{ \begin{array}{c} \dot{x}_{ac} \\ \dot{x}_{cs} \end{array} \right\} = \left[\begin{array}{cc} A_{11} & A_{12} \\ A_{21} & A_{22} \end{array} \right] \left\{ \begin{array}{c} x_{ac} \\ x_{cs} \end{array} \right\} + \left[\begin{array}{c} B_1 \\ B_2 \end{array} \right] \{\delta\} \quad (146)$$

$$\{y_{ac}\} = \left[\begin{array}{cc} C_1 & C_2 \end{array} \right] \left\{ \begin{array}{c} x_{ac} \\ x_{cs} \end{array} \right\} + [D_1]\{\delta\} \quad (147)$$

where,

$$A_{11} = A + B\Pi \quad (148)$$
$$A_{12} = B\Upsilon \quad (149)$$
$$A_{21} = H + E(A + B\Pi) \quad (150)$$
$$A_{22} = F + EB\Upsilon \quad (151)$$
$$B_1 = B\Xi \quad (152)$$
$$B_2 = G + EB\Xi \quad (153)$$
$$C_1 = C + D\Pi \quad (154)$$
$$C_2 = D\Upsilon \quad (155)$$
$$D_1 = D\Xi \quad (156)$$
$$\Pi = [I - ZB]^{-1}(R + ZA) \quad (157)$$
$$\Upsilon = [I - ZB]^{-1} P \quad (158)$$
$$\Xi = [I - ZB]^{-1} Q \quad (159)$$

Concluding Remarks

A linear coupled rotor-fuselage-control system dynamic model is presented in this paper. The model is expected to be useful for flying qualities studies, stability and control investigations, and control design parametric studies. Efforts are underway to produce numerical results for the validation of the model.

References

[1] Miller, D.G., and White, F., "A Treatment of the Impact of Rotor-Fuselage Coupling on Helicopter Handling Qualities," Proceedings of the 43rd Annual Forum of the American Helicopter Society, St. Louis, MO, May 1987.

[2] Talbot, P.D., Tinling, B.E., Decker, W.A., and Chen, R.T.N., "A Mathematical Model of a Single Main Rotor Helicopter for Piloted Simulation," NASA TM 84281, September 1982.

[3] Gibbons, M.P., and Done, G.T.S., "Automatic Generation of Helicopter Rotor Aeroelastic Equations of Motion," *Vertica*, Vol. 8, No. 3, pp. 229-241, 1984.

[4] Lytwyn, R.T., "Aeroelastic Stability Analysis of Hingeless Rotor Helicopters in Forward Flight Using Blade and Airframe Normal Modes," Proceedings of the 36th Annual Forum of the American Helicopter Society, Washington DC, May 1980.

[5] Zhao X., and Curtiss H.C., "A Linearized Model of Helicopter Dynamics Including Correlation with Flight Test," Proceedings of the Second International Conference on Rotorcraft Basic Research, University of Maryland, College Park, Maryland, 1988.

[6] McKillip R., Curtiss H.C., "Approximations for Inclusion of Rotor Lag Dynamics in Helicopter Flight Dynamics Models," Proceedings of the Seventeenth European Rotorcraft Forum, Berlin, Germany, September 1991.

[7] Kane, T.R., and Levinson, D.A., *Dynamics: Theory and Applications*, McGraw Hill Book Company, 1985.

[8] Pitt, D.M., and Peters, D.A., "Theoretical Prediction of Dynamic Inflow Derivatives," *Vertica* Vol. 5, pp. 21-34, 1981.

[9] Prouty, R.W., *Helicopter Performance, Stability, and Control*, PWS Publishers, 1986, pp. 379-441.

[10] Johnson, W., *Helicopter Theory*, Princeton University Press, 1980, pp. 213-216.

[11] Hohenemser K.H., and Yin, S.K., "Some Applications of the Method of Multiblade Coordinates," *Journal of the American Helicopter Society*, Vol. 17, No. 3, July 1972, pp. 3-12.

[12] Peters, D.A., HaQuang N., "Dynamic Inflow for Practical Applications," *Journal of the American Helicopter Society*, Volume 33, Number 4, October 1988.

[13] Gill, P.E., Murray, W., and Wright, M.H., *Practical Optimization*, Academic Press, 1989, pp. 105-115.

Appendix

Skew-Symmetric Matrix Operator

For a vector $a = \{a_1, a_2, a_3\}^T$, the matrix $S(a)$ is defined as,

$$S(a) = \begin{bmatrix} 0 & -a_3 & a_2 \\ a_3 & 0 & -a_1 \\ -a_2 & a_1 & 0 \end{bmatrix}$$

Single Axis Transformation Matrices

The matrices E_1, E_2, and E_3 represent single axis transformations about x, y, and z axes, respectively, and are defined as follows:

$$E_1(\kappa) = \begin{bmatrix} 1 & 0 & 0 \\ 0 & \cos\kappa & \sin\kappa \\ 0 & -\sin\kappa & \cos\kappa \end{bmatrix}$$

$$E_2(\kappa) = \begin{bmatrix} \cos\kappa & 0 & -\sin\kappa \\ 0 & 1 & 0 \\ \sin\kappa & 0 & \cos\kappa \end{bmatrix}$$

$$E_3(\kappa) = \begin{bmatrix} \cos\kappa & \sin\kappa & 0 \\ -\sin\kappa & \cos\kappa & 0 \\ 0 & 0 & 1 \end{bmatrix}$$

Time-Derivative of a Transformation Matrix

Consider the time-derivative of a vector v in two reference frames denoted by A and B. Let the components of v in Frame A be denoted by v_A and those in Frame B be denoted by v_B. Let the angular velocity of Frame B with respect to Frame A be ω and let the components of ω in Frame B be denoted by ω_B. Let T represent the transformation matrix that transforms vector components from Frame B axes to components in Frame A axes. The time-derivatives of v in Frame A and Frame B are related by the following vectorial equation:

$${}^A\frac{dv}{dt} = {}^B\frac{dv}{dt} + \omega \times v$$

In matrix-vector format, the preceding equation can be written as,

$$\dot{v}_A = T\dot{v}_B + TS(\omega_B)v_B$$

Also, since $v_A = Tv_B$, one gets for $\dot{v}_A$ the following expression:

$$\dot{v}_A = T\dot{v}_B + \dot{T}v_B$$

Comparing the two equations for $\dot{v}_A$, the following formula is obtained for $\dot{T}$:

$$\dot{T} = TS(\omega_B)$$

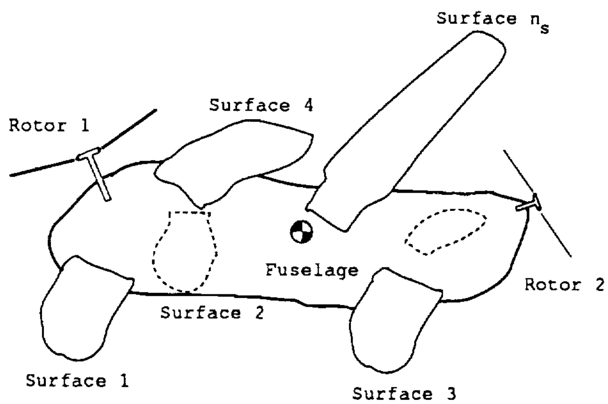

Figure 1: Generic Rotorcraft Configuration

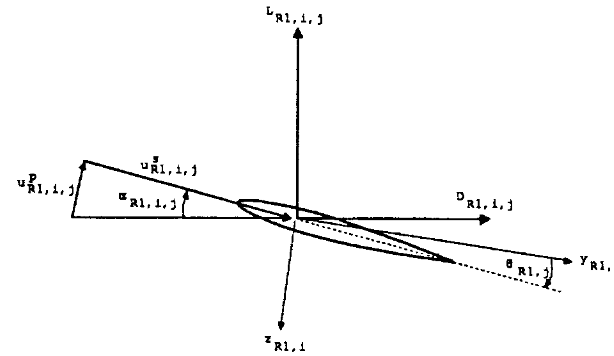

Figure 3: jth Aerodynamic Element of the ith Rotor 1 Blade

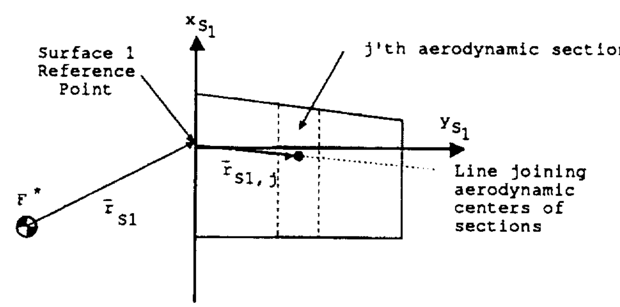

Figure 4: External Surface Aerodynamic Sections

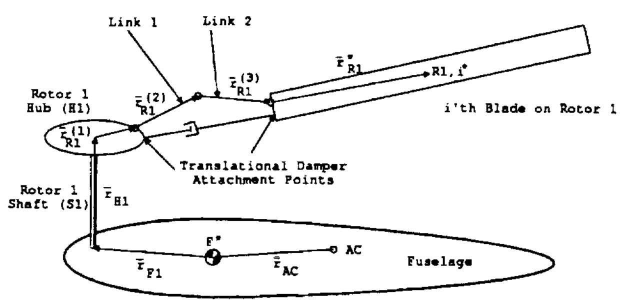

Figure 2: Rotor Blade Geometry

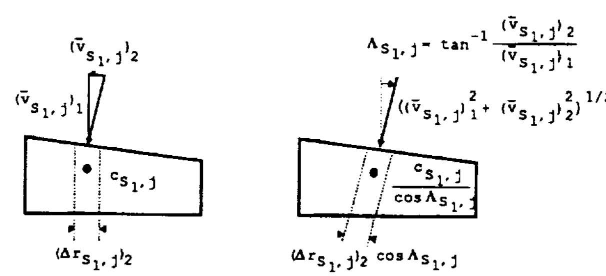

Figure 5: jth Aerodynamic Section of Surface 1 in Yawed Free Stream

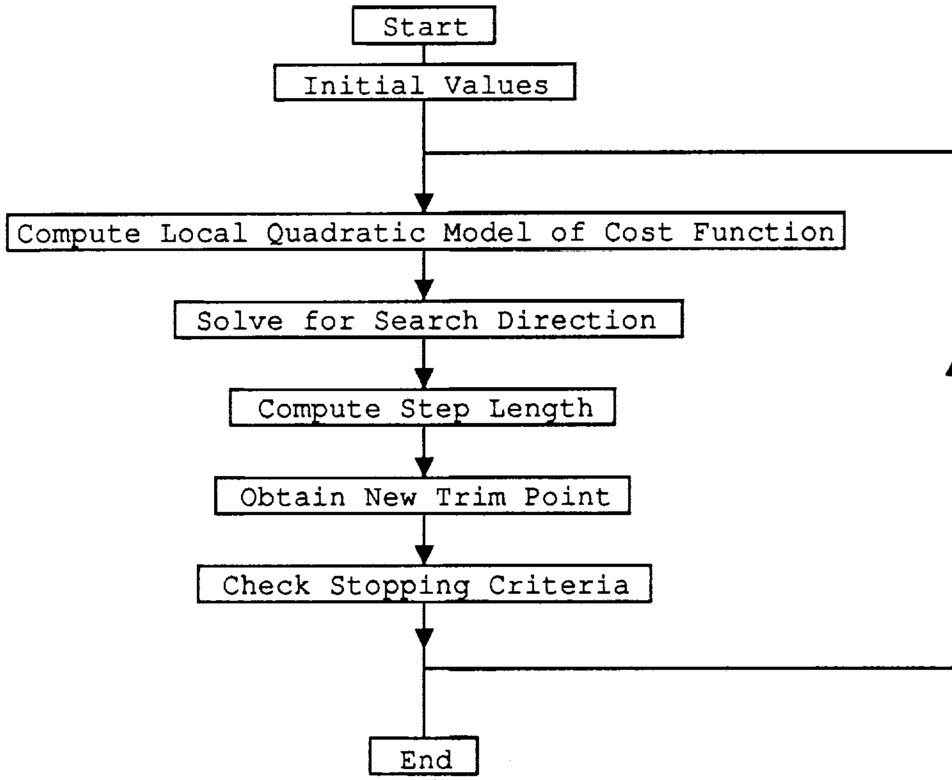

Figure 6: Trim Procedure Flowchart

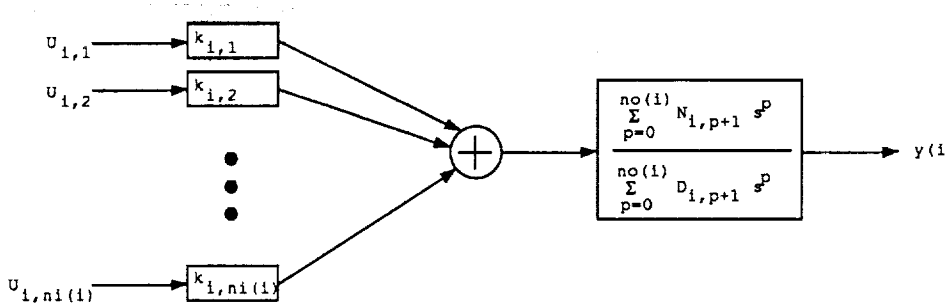

ni(i) = Number of Inputs to i'th Filter

no(i) = Order of i'th Filter

y(i) = Output of i'th Filter

$k_{i,j}$ = Gain Multiplying j'th input of i'th Filter

Figure 7: ith Flight Control System Filter